

# Physics of Autonomous Driving based on Three-Phase Traffic Theory

Boris S. Kerner<sup>1</sup>

<sup>1</sup> *Physics of Transport and Traffic, University Duisburg-Essen, 47048 Duisburg, Germany*

We have revealed physical features of autonomous driving in the framework of the three-phase traffic theory for which there is *no* fixed time headway to the preceding vehicle. A comparison with the classical model approach to autonomous driving for which an autonomous driving vehicle tries to reach a fixed (desired or “optimal”) time headway to the preceding vehicle has been made. It turns out that autonomous driving in the framework of the three-phase traffic theory exhibits the following advantages in comparison with the classical model of autonomous driving: (i) The absence of string instability. (ii) Considerably smaller speed disturbances at road bottlenecks. (iii) Autonomous driving vehicles based on the three-phase theory decrease the probability of traffic breakdown at the bottleneck in mixed traffic flow consisting of human driving and autonomous driving vehicles; on the contrary, even a single autonomous driving vehicle based on the classical approach can provoke traffic breakdown at the bottleneck in mixed traffic flow.

PACS numbers: 89.40.-a, 47.54.-r, 64.60.Cn, 05.65.+b

It is generally assumed that future vehicular traffic is a mixed traffic flow consisting of human driving and autonomous driving vehicles [1–9]. Autonomous driving vehicles should considerably enhance capacity of a traffic network that is limited by traffic breakdown at network bottlenecks. For an analysis of the dynamics of autonomous driving vehicles and its effect on traffic flow, we consider a simple case of vehicular traffic on a single-lane road with an on-ramp bottleneck. On the single-lane road, no vehicles can pass. For this reason, autonomous driving can be achieved through the use of an adaptive cruise control (ACC) in a vehicle: An ACC-vehicle follows the preceding vehicle (that can be either a human driving vehicle or an ACC-vehicle) automatically based on some ACC dynamics rules of motion. In a classical ACC model, acceleration (deceleration)  $a^{(\text{ACC})}$  of the ACC vehicle is determined by the space gap to the preceding vehicle  $g$  and the relative speed  $\Delta v = v_\ell - v$  measured by the ACC vehicle as well as by a desired time headway  $\tau_d^{(\text{ACC})}$  of the ACC-vehicle to the preceding vehicle (Fig. 1 (a)) (see, e.g., [2–9] and references there):

$$a^{(\text{ACC})} = K_1(g - v\tau_d^{(\text{ACC})}) + K_2(v_\ell - v), \quad (1)$$

where  $v$  is the speed of the ACC-vehicle,  $v_\ell$  is the speed of the preceding vehicle; here and below  $v$ ,  $v_\ell$ , and  $g$  are time-functions;  $K_1$  and  $K_2$  are coefficients of ACC adaptation. It is well-known that there can be string instability of a long enough platoon of ACC-vehicles (1) [2–9] that occurs under condition  $K_2 < (2 - K_1(\tau_d^{(\text{ACC})})^2)/2\tau_d^{(\text{ACC})}$  found by Liang and Peng [3].

However, there is another basic physical problem of the classical autonomous driving: Even when the above-mentioned condition for string instability is not satisfied, i.e., any platoon of ACC-vehicles is stable, already a small share of ACC-vehicles in mixed traffic flow can deteriorate traffic while provoking traffic breakdown at network bottlenecks [10].

A study of real field traffic data shows [11] that the basic feature of classical autonomous driving systems – a

desired time headway is fundamentally inconsistent with a basic behavior of real drivers. To explain the empirical data, in the three-phase traffic theory is assumed when a driver approaches a slower moving preceding vehicle and the driver cannot pass it, the driver decelerates within a synchronization space gap  $G$  adapting the speed to the speed of the preceding vehicle without caring what the precise space gap  $g$  to the preceding vehicle is as long as it is not smaller than a safe space gap  $g_{\text{safe}}$  [11]. This speed adaptation occurs within the synchronization space gap that limits a 2D-region of synchronized flow states (dashed region in Fig. 1 (b)) determined by conditions

$$g_{\text{safe}} \leq g \leq G. \quad (2)$$

In other words, accordingly to (2), drivers do not try to reach a particular (desired or optimal) time headway to the preceding vehicle, but adapt the speed while keeping time headway  $\tau^{(\text{net})} = g/v$  in a range  $\tau_{\text{safe}} \leq \tau^{(\text{net})} \leq \tau_G$ , where  $\tau_G = G/v$ ,  $\tau_G$  is a synchronization time headway,  $\tau_{\text{safe}} = g_{\text{safe}}/v$  is a safe time headway and it is assumed that the speed  $v > 0$ . In inventions [12], we have assumed that to satisfy these empirical features of real traffic, acceleration (deceleration) of autonomous driving based on the three-phase theory (for short, three-traffic-phase ACC – TPACC) should be given by formula [12]

$$a^{(\text{TPACC})} = K_{\Delta v}(v_\ell - v) \quad \text{at } g_{\text{safe}} \leq g \leq G \quad (3)$$

where  $K_{\Delta v}$  is a dynamic coefficient ( $K_{\Delta v} > 0$ ).

However, no studies of autonomous driving based on the three-phase theory have been done up to now, and, therefore, the physics of TPACC has not been known. In this Letter, we reveal the physical features of TPACC and the effect of TPACC-vehicles on mixed traffic flow as well as compare TPACC with autonomous driving based on the classical approach.

To understand physical features of autonomous driving in the framework of the three-phase theory, we introduce

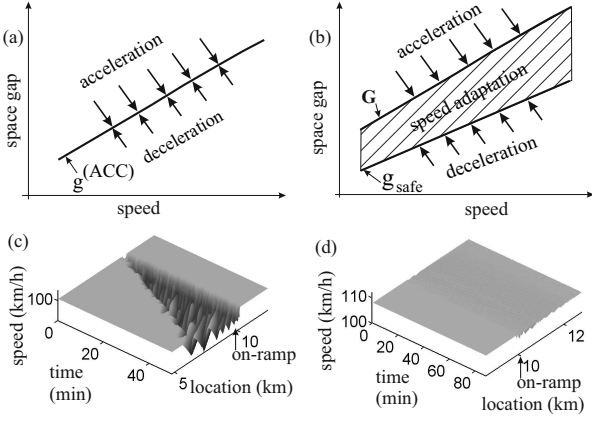


FIG. 1: String instability of the classical ACC model (1) (see a version of ACC model with discrete time used for simulations in [10]) (a, c) and string stability of TPACC model (5)–(7) (b, d) in traffic flow consisting of 100% of autonomous driving vehicles on a single-lane road with on-ramp bottleneck located at  $x = 10$  km: (a) Qualitative speed dependence of desired space gap  $g^{(ACC)} = v\tau_d^{(ACC)}$  of ACC for which at a given speed there is a single operating point  $g = g^{(ACC)}$  (see, e.g., [2–9]). (b) Qualitative presentation of a part of 2D-region for operating points of TPACC in the space-gap–speed plane: at a given speed of TPACC-vehicle there are the infinity of operating points of TPACC [12]. (c, d) Simulations of string instability of ACC at on-ramp bottleneck with the classical ACC model (1) with discrete time [10] (c) and string stability of TPACC at on-ramp bottleneck with the TPACC model (5)–(7) (d): Speed in space and time. Simulation parameters of ACC (c) and TPACC (d) are identical ones: the on-ramp inflow rate  $q_{on} = 320$  vehicles/h and the flow rate upstream of the bottleneck  $q_{in} = 2002.6$  vehicles/h,  $\tau_d^{(ACC)} = \tau_p = 1.3$  s,  $\tau_G = 1.4$  s,  $K_1 = 0.3$  s $^{-2}$  and  $K_2 = K_{\Delta v} = 0.3$  s $^{-1}$ ;  $a_{max} = b_{max} = 3$  m/s $^2$ ,  $v_{free} = 30$  m/s (108 km/h), vehicle length  $d = 7.5$  m. In accordance with the desired time headway  $\tau_d^{(ACC)} = 1.3$  s of the ACC-vehicles, the sum flow rate  $q_{sum} = q_{in} + q_{on} = 2322.6$  vehicles/h is related to time headway 1.3 s between vehicles in free flow.

the following TPACC model:

$$a^{(TPACC)} = \begin{cases} K_{\Delta v}(v_\ell - v) & \text{at } g \leq G \\ K_1(g - v\tau_p) + K_2(v_\ell - v) & \text{at } g > G, \end{cases} \quad (4)$$

where  $\tau_p$  is a model parameter and it is assumed that  $g \geq g_{safe}$ . All simulations of human driving vehicles in mixed traffic flow are made below with the Kerner-Klenov microscopic stochastic model with discrete time  $t = n\tau$ , where  $n = 0, 1, 2, \dots$ ;  $\tau = 1$  s is time step [13]. For this reason, we simulate TPACC-model (4) with discrete time  $t = n\tau$ . Respectively, TPACC-model (4) should be rewritten as follows:

$$a_n^{(TPACC)} = \begin{cases} K_{\Delta v}(v_{\ell,n} - v_n) & \text{at } g_n \leq G_n \\ K_1(g_n - v_n\tau_p) + K_2(v_{\ell,n} - v_n) & \text{at } g_n > G_n, \end{cases} \quad (5)$$

where  $G_n = v_n\tau_G$ . When  $g_n < g_{safe,n}$ , the TPACC-

vehicle should move in accordance with some safety conditions to avoid collisions between vehicles (Fig. 1 (b)). A collision-free TPACC-vehicle motion is described as made in [10] for the classical model of ACC:

$$v_{c,n}^{(TPACC)} = v_n + \tau \max(-b_{max}, \min(\lfloor a_n^{(TPACC)} \rfloor, a_{max})), \quad (6)$$

$$v_{n+1} = \max(0, \min(v_{free}, v_{c,n}^{(TPACC)}, v_{s,n})), \quad (7)$$

where  $\lfloor z \rfloor$  denotes the integer part of  $z$  (note that Eqs. (6), (7) for TPACC are the same as those for the classical ACC model with discrete time considered in [10]); the TPACC acceleration and deceleration are limited by  $a_{max}$  and  $b_{max}$ , respectively; the speed  $v_{n+1}$  (7) at time step  $n + 1$  is limited by the maximum speed  $v_{free}$  and by the safe speed  $v_{s,n}$  that have been chosen, respectively, the same as those in the model of human driving vehicles [13], a discrete version of the classical ACC model [10], the model of the on-ramp bottleneck as well as model parameters used in simulations have been reviewed in Appendix A of the book [14].

In accordance with Eq. (7), condition  $v_{c,n}^{(TPACC)} \leq v_{s,n}$  is equivalent to condition  $g_n \geq g_{safe,n}$ . Under this condition, from (5)–(7) it follows that when time headway  $\tau_n^{(net)} = g_n/v_n$  of the TPACC-vehicle to the preceding vehicle is within the range

$$\tau_{safe,n} \leq \tau_n^{(net)} \leq \tau_G, \quad (8)$$

the acceleration (deceleration) of the TPACC-vehicle does not depend on time headway, where  $\tau_{safe,n} = g_{safe,n}/v_n$  is a safe time headway and it is assumed that  $v_n > 0$ . Thus, in contrast with the classical ACC model (1) (Fig. 1 (a)), there is *no* fixed desired time headway to the preceding vehicle for the autonomous driving vehicle based on the three-phase theory (Fig. 1 (b)).

The speed adaptation within the 2D-traffic flow states of the three-phase theory used in TPACC model (5)–(7) changes the dynamic behavior of autonomous driving basically in comparison with the classical ACC model (1).

Simulations of string instability of ACC-vehicles are shown in Fig. 1 (c). Speed disturbances in traffic flow consisting of 100% ACC-vehicles occur at an on-ramp bottleneck at which on-ramp inflow with the rate  $q_{on}$  and upstream flow with the rate  $q_{in}$  merge. String instability of ACC-vehicles leads to the emergence of moving jams upstream of the bottleneck (Fig. 1 (c)). Contrarily, at the same set of the flow rates  $q_{on}$  and  $q_{in}$  as well as the same other model parameters *no* string instability of any platoon of the TPACC-vehicles is realized: In Fig. 1 (d), all speed disturbances occurring at the bottleneck decay upstream of the bottleneck. It turns out that as long as time headway between TPACC-vehicle is within the range (8), speed disturbances decay over time. This is because within this range the acceleration (deceleration) of TPACC-vehicle does not depend on time headway.

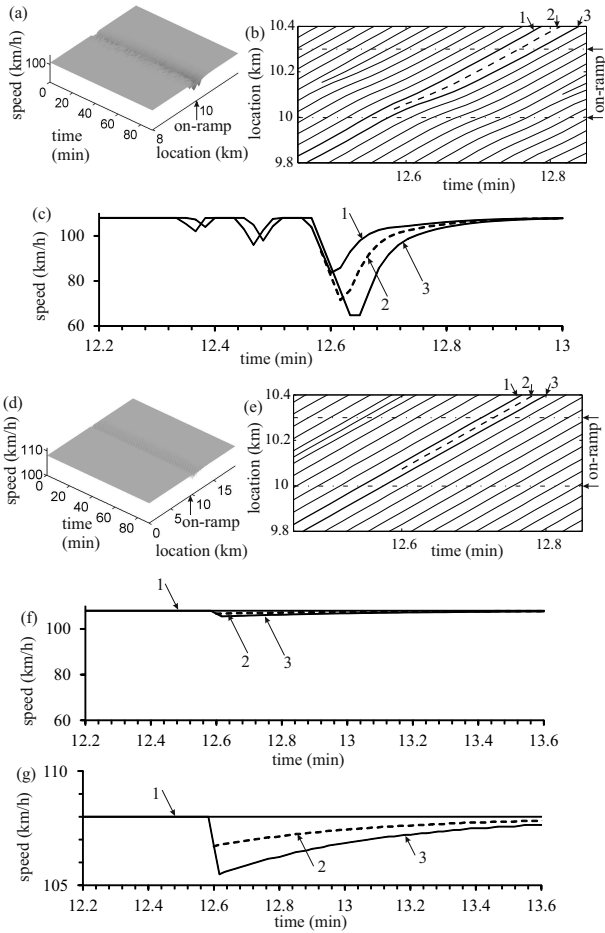


FIG. 2: Speed disturbances at on-ramp bottleneck in stable free flow with 100% autonomous driving vehicles for classical ACC model (1) (see a version of ACC model with discrete time used for simulations in [10]) (a–c) and for TPACC model (5)–(7) (d–g): (a, d) Speed in space and time. (b, e) Fragments of vehicle trajectories; (b) is related to (a) and (e) is related to (d). (c, f, g) Microscopic speeds along vehicle trajectories shown by, respectively, the same numbers in (b, e); (c) is related to (b) and (f, g) are related to (e); (f) and (g) show the same speed in different speed-scales. Simulation parameters of ACC (a–c) and TPACC (d–g) are identical ones.  $K_2 = K_{\Delta v} = 0.6 \text{ s}^{-1}$ . Other model parameters are the same as those in Fig. 1.

At a larger value of  $K_2$  in (1) as well as at the same desired time headway  $\tau_d^{(\text{ACC})} = 1.3 \text{ s}$  and the same set of the flow rates  $q_{\text{on}}$  and  $q_{\text{in}}$  as those in Fig. 1, platoons of ACC-vehicles become stable (Fig. 2 (a)). However, it turns out that considerable speed disturbances appear at the bottleneck. This case is shown in Fig. 2 (b, c) in which ACC-vehicle 2 merges from the on-ramp onto the main road following ACC-vehicle 1 moving on the main road. To satisfy the desired time headway  $\tau_d^{(\text{ACC})}$ , ACC-vehicle 2 should decelerate to a lower speed than the minimum speed of ACC-vehicle 1. This deceleration

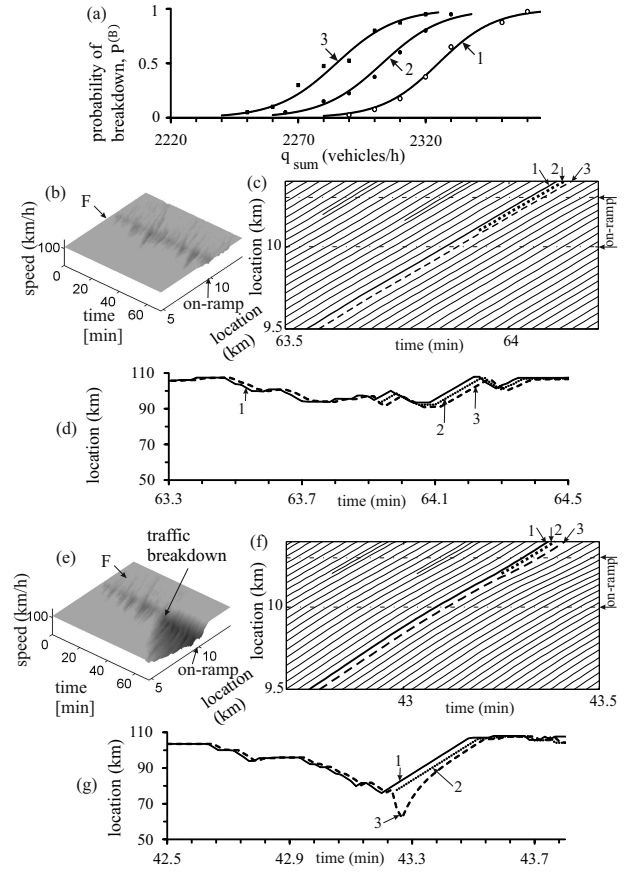


FIG. 3: Effect of a single autonomous driving vehicle on the probability of traffic breakdown in mixed traffic flow with only 2% of autonomous driving vehicles: (a) Probability of traffic breakdown at on-ramp bottleneck as a function of the flow rate  $q_{\text{sum}} = q_{\text{in}} + q_{\text{on}}$  at a given flow rate  $q_{\text{in}} = 2000 \text{ vehicles/h}$ ; curve 1 is related to traffic flow without autonomous driving vehicles as well as to mixed traffic flow with TPACC-vehicles; curves 2 and 3 are related to mixed traffic flow with ACC-vehicles, respectively, with  $\tau_d^{(\text{ACC})} = 1.3 \text{ s}$  and  $1.6 \text{ s}$ . (b–g) Speed disturbances occurring at on-ramp bottleneck through a single TPACC-vehicle (b–d) and a single ACC-vehicle (e–g): (b, e) Speed in space and time; F – free flow. (c, f) Fragments of vehicle trajectories. (d, g) Microscopic speeds along vehicle trajectories shown by the same numbers in (c, f), respectively. In (c, d, f, g), vehicles 1 and 2 are manual driving vehicles whereas vehicle 3 is ACC-vehicle in (c, d) and TPACC-vehicle in (f, g). In (b–g),  $q_{\text{in}} = 2000 \text{ vehicles/h}$ ,  $q_{\text{on}} = 280 \text{ vehicles/h}$ ; other model parameters for ACC-vehicles and TPACC-vehicles are, respectively, the same as those in Fig. 2.

of ACC-vehicle 2 forces the following ACC-vehicle 3 to decelerate while approaching ACC-vehicle 2. Simulations show that the occurrence of large speed disturbances at the bottleneck is a basic problem of ACC-vehicles based on the classical approach in which the ACC-vehicles try to reach a desired time headway  $\tau_d^{(\text{ACC})}$ .

These large speed disturbances at the bottleneck caused by ACC-vehicles (Fig. 2 (b, c)) do not occur in

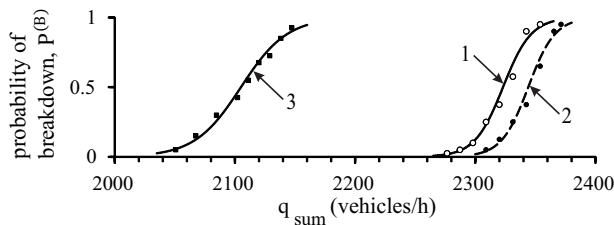


FIG. 4: Probability of traffic breakdown at on-ramp bottleneck as a function of the flow rate  $q_{\text{sum}} = q_{\text{in}} + q_{\text{on}}$  at a given on-ramp inflow rate  $q_{\text{on}} = 320$  vehicles/h in mixed traffic flow with 20% autonomous driving vehicles: Curve 1 is related to traffic flow without autonomous driving vehicles. Curves 2 and 3 are related to mixed traffic flow with TPACC-vehicles (curve 2) and ACC-vehicles (curve 3). Simulation parameters of ACC and TPACC are, respectively, the same as those in Fig. 2.

traffic flow consisting of TPACC-vehicles (Fig. 2 (d–g)). This is because within the range of time headway (8) the acceleration (deceleration) of an TPACC-vehicle does not depend on time headway. This explains small amplitudes of speed disturbances caused by TPACC-vehicles 2 and 3 at the bottleneck (Fig. 2 (e, f, g)). The speed disturbances caused by TPACC-vehicles are so small (Fig. 2 (f)) that in the same speed-scale as that used for the classical ACC (Fig. 2 (c)) they cannot almost be resolved. Only at considerably larger speed-scale the speed disturbances become visible (Fig. 2 (g)).

Traffic breakdown in a flow of manual driving vehicles is a phase transition from free flow (F) to synchronized flow (S) ( $F \rightarrow S$  transition) occurring in a metastable free flow with respect to the  $F \rightarrow S$  transition. The larger the amplitude of speed disturbances at the bottleneck, the more probable the nucleus occurrence for the breakdown, i.e., the larger the probability of traffic breakdown  $P^{(B)}$  at the bottleneck [10, 11].

In the next future, we could expect a mixed traffic flow in which the share of autonomous driving vehicles is small (Fig. 3). Single TPACC-vehicles moving in a such mixed traffic flow cause very small speed disturbances at the bottleneck (Fig. 3 (b–d)). Indeed, we have found that probability of traffic breakdown remains in

this mixed flow the same as that in traffic flow consisting of manual drivers only (curve 1 in Fig. 3 (a)). Contrarily, probability of traffic breakdown can increase even when a very small amount of classical ACC-vehicles is in a mixed traffic flow (curves 2 and 3 in Fig. 3 (a)). This deterioration of traffic through classical autonomous driving is explained by the occurrence of a large amplitude speed disturbance caused by a classical ACC-vehicle at the bottleneck (Fig. 3 (e–g)): Already a single ACC-vehicle can initiate traffic breakdown at the bottleneck (Fig. 3 (e–g)).

If the share of autonomous driving vehicles in mixed traffic flow increases (Fig. 4), the probability of traffic breakdown caused by ACC-vehicles that deteriorate traffic can increase considerably (Fig. 4, curve 3). Contrarily, long enough platoons of TPACC-vehicles in mixed traffic flow decrease the breakdown probability (Fig. 4, curve 2). This physical feature of TPACC-vehicles is also explained by the speed adaptation effect of the three-phase theory that is the basis of TPACC (4): At each vehicle speed, the TPACC-vehicle makes an arbitrary choice in time headway that satisfies conditions (8). In other words, the TPACC-vehicle accepts different values of time headway at different times and does not control a fixed time headway to the preceding vehicle.

By autonomous driving in the framework of the three-phase theory (TPACC) there is *no* fixed desired time headway to the preceding vehicle. In the Letter, we have shown that this physical feature of TPACC leads to the following advantages in comparison with the classical approach to autonomous driving: (i) The absence of string instability. (ii) Considerably smaller speed disturbances at road bottlenecks. (iii) Autonomous driving vehicles based on the three-phase theory decrease the probability of traffic breakdown at the bottleneck in mixed traffic flow; on the contrary, even a single autonomous driving vehicle based on the classical approach can provoke traffic breakdown at the bottleneck in mixed traffic flow.

I would like to thank Sergey Klenov for help and useful suggestions. We thank our partners for their support in the project “MEC-View – Object detection for automated driving based on Mobile Edge Computing”, funded by the German Federal Ministry of Economic Affairs and Energy.

- 
- [1] Autonomous driving vehicles are also called automated driving or automatic driving or else self-driving vehicles. Under automated driving or automatic driving vehicles are often understood autonomous driving vehicles that are connected each other (vehicle-to-vehicle (V2V) communication) or/and with infrastructure (V2X communication).
  - [2] W. Levine, M. Athans, *IEEE Trans. Automat. Contr.* **11** 355–361 (1966).
  - [3] C.-Y. Liang, H. Peng, *Veh. Syst. Dyn.* **32** 313–330 (1999).
  - [4] C.-Y. Liang, H. Peng, *JSME Jnt. J. Ser. C* **43** 671–677 (2000).
  - [5] R. Rajamani, *Vehicle Dynamics and Control, Mechanical Engineering Series*, (Springer US, Boston, MA, 2012).
  - [6] D. Swaroop, J.K. Hedrick, *IEEE Trans. Automat. Contr.* **41** 349–357 (1996).
  - [7] D. Swaroop, J.K. Hedrick, S.B. Choi, *IEEE Trans. Veh. Technol.* **50** 150–161 (2001).
  - [8] L.C. Davis, *Phys. Rev. E* **69** 066110 (2004).
  - [9] L.C. Davis, *Physica A* **405** 128–139 (2014).
  - [10] B.S. Kerner, *Physica A* **450** 700–747 (2016).
  - [11] B.S. Kerner, *Phys. Rev. Lett.* **81** 3797–3800 (1998); B.S.

- Kerner, *Trans. Res. Rec.* **1678** 160–167 (1999); B.S. Kerner, in *Transportation and Traffic Theory*, ed. by A. Ceder. (Elsevier Science, Amsterdam, 1999), pp. 147–171; B.S. Kerner, *Physics World* **12** 25–30 (August 1999); B.S. Kerner, *The Physics of Traffic* (Springer, Berlin, New York 2004); B.S. Kerner, *Introduction to Modern Traffic Flow Theory and Control*. (Springer, Berlin, New York, 2009).
- [12] B.S. Kerner, German patent publication DE 10308256A1 (2004); B.S. Kerner, Patent WO 2004076223A1 (2004); B.S. Kerner, EU Patent EP 1597106B1 (2006); B.S. Kerner, German patent DE 502004001669D1 (2006); B.S. Kerner, USA patent US 20070150167A1 (2007); B.S. Kerner, USA patent US 7451039B2 (2008); B.S. Kerner, German patent publication DE 102007008253A1 (2007); B.S. Kerner, German patent publication DE 102007008257A1 (2007); B.S. Kerner, German patent publication DE 102007008254A1 (2008).
- [13] B.S. Kerner, S.L. Klenov, *J. Phys. A: Math. Gen.* **35**, L31–L43 (2002); B.S. Kerner, S.L. Klenov, *Phys. Rev. E* **68**, 036130 (2003); B.S. Kerner, S.L. Klenov, **80**, 056101 (2009).
- [14] B.S. Kerner, *Breakdown in Traffic Networks* (Springer, Berlin, New York 2017).